Supplementary Figures 1-11

Acsbg1 maintains intestinal immune homeostasis and controls inflammation by regulating ST2^{+} Tregs

Martina Palatella, Friederike Kruse, Honglei Ji, Alina Langenhagen, Maike Becker, Carolin Daniel, Maria Rohm, Jochen Huehn

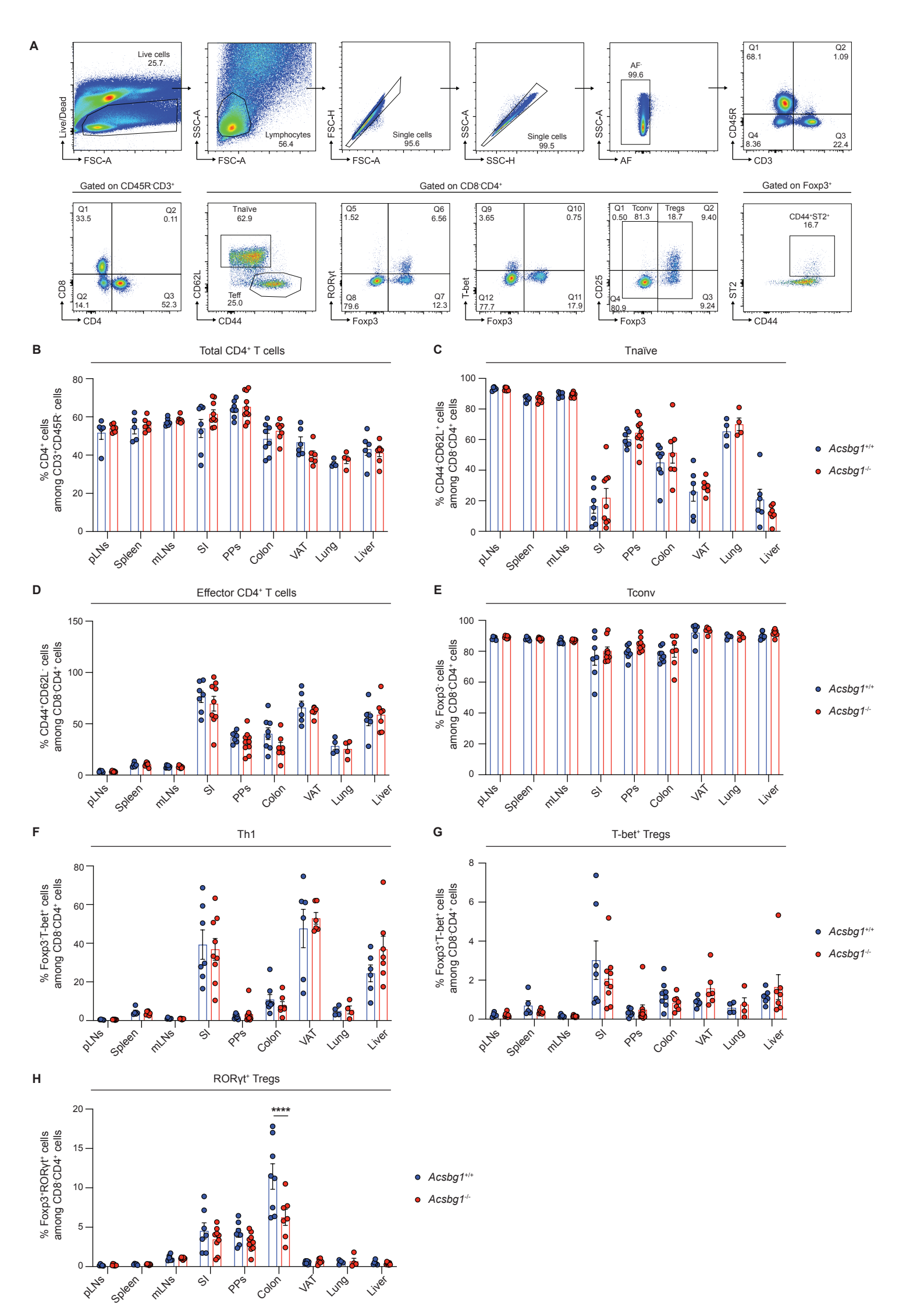
A
Live cells
25.7
Live/Dead
FSC-A
SSC-A
Lymphocytes
56.4
FSC-A
FSC-H
Single cells
95.6
FSC-A
SSC-A
Single cells
99.5
SSC-H
AF⁻
99.6
AF
SSC-A
Q1
68.1
Q2
1.09
Q4
8.36
Q3
22.4
CD45R
CD3
Gated on CD45R⁻CD3⁺
Q1
33.5
Q2
0.11
Q2
14.1
Q3
52.3
CD8
CD4
Gated on CD8⁻CD4⁺
Tnaïve
62.9
Teff
25.0
CD62L
CD44
Q5
1.52
Q6
6.56
Q8
79.6
Q7
12.3
RORγt
Foxp3
Q9
3.65
Q10
0.75
Q12
77.7
Q11
17.9
T-bet
Foxp3
Q1
0.50
Tconv
81.3
Tregs
18.7
Q2
9.40
Q4
80.9
Q3
9.24
CD25
Foxp3
Gated on Foxp3⁺
CD44⁺ST2⁺
16.7
ST2
CD44
B
Total CD4⁺ T cells
% CD4⁺ cells among CD3⁺CD45R⁻ cells
pLNs
Spleen
mLNs
SI
PPs
Colon
VAT
Lung
Liver
C
Tnaïve
% CD44⁻CD62L⁺ cells among CD8⁻CD4⁺ cells
Acsbg1+/+
Acsbg1-/-
D
Effector CD4⁺ T cells
% CD44⁺CD62L⁻ cells among CD8⁻CD4⁺ cells
E
Tconv
% Foxp3⁻ cells among CD8⁻CD4⁺ cells
F
Th1
% Foxp3⁻T-bet⁺ cells among CD8⁻CD4⁺ cells
G
T-bet⁺ Tregs
% Foxp3⁺T-bet⁺ cells among CD8⁻CD4⁺ cells
H
RORγt⁺ Tregs
****
% Foxp3⁺RORγt⁺ cells among CD8⁻CD4⁺ cells

Supplementary Figure 1. *Acsbg1* deficiency affects the composition of CD4$^+$ T cell subsets in adult mice. (A) Gating strategy for immunophenotyping. Live/dead discrimination was performed using the LIVE/DEAD Fixable Blue Dead Cell Stain. Live cells were gated according to the forward scatter (FSC) and side scatter (SSC) area parameters. Doublet exclusion was performed using the height (H) versus width (W) parameters of FSC and SSC, respectively, and autofluorescent (AF) cells were excluded. CD45R$^-$CD3$^+$ cells were gated to identify T cells. CD45R$^-$CD3$^+$ T cells were then further subdivided into CD4$^+$ and CD8$^+$ T cells. According to the expression of Foxp3, CD4$^+$ T cells were subclassified into Foxp3$^+$ Tregs and Foxp3$^-$ Tconv. CD25 expression was also evaluated in both Foxp3$^+$ Tregs and Foxp3$^-$ Tconv. According to the expression of Foxp3 in combination with that of the master transcription factors T-bet or RORγt, T-bet$^+$ Th1 and RORγt$^+$ Th17 cells, RORγt$^+$ Tregs and T-bet$^+$ Tregs were gated within the CD4$^+$ T cell population. The CD4$^+$ Tnaïve and effector/memory subpopulations were also analyzed for the expression of CD44 and CD62L. In addition, CD44$^+$ST2$^+$ cells were gated among the Foxp3$^+$ Tregs. **(B-H)** Summary graphs of immunophenotyping performed in pLNs, spleen, mLNs, SI, PPs, colon, VAT, lung and liver of adult 7-10 week old *Acsbg1*$^{-/-}$ mice and *Acsbg1*$^{+/+}$ littermate controls. **(B)** Frequency of total CD4$^+$ cells among CD3$^+$ T cells. Frequencies of **(C)** CD44$^-$CD62L$^+$ naïve, **(D)** CD44$^+$CD62L$^-$ effector, **(E)** Foxp3$^-$ Tconv, **(F)** Foxp3$^-$T-bet$^+$ Th1, **(G)** T-bet$^+$ Tregs (Foxp3$^+$T-bet$^+$) and **(H)** RORγt$^+$ Tregs (Foxp3$^+$RORγt$^+$) among CD8$^-$CD4$^+$ T cells. Each symbol represents a single mouse. Data are presented as mean ± SEM. Results were pooled from 6 independent experiments with 4-10 mice per experimental group. Significance of differences between means was assessed by ordinary two-way ANOVA with Šídák's multiple comparison test (mean ± 95% CI; **P*<0.05, ***P*<0.01, ****P*<0.001).

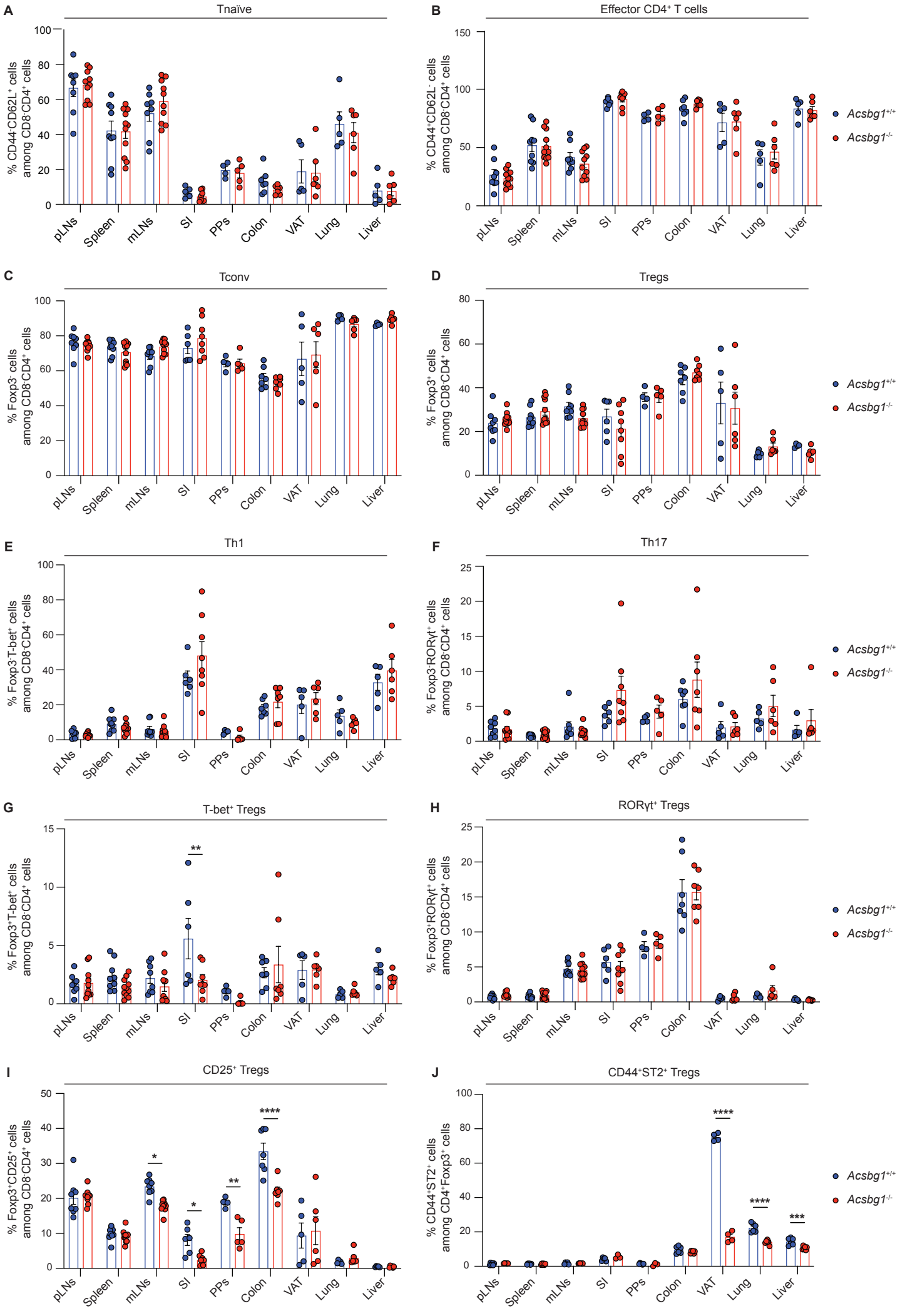
A
Tnaïve
% CD44+CD62L+ cells among CD8-CD4+ cells
B
Effector CD4+ T cells
% CD44+CD62L- cells among CD8-CD4+ cells
C
Tconv
% Foxp3- cells among CD8-CD4+ cells
D
Tregs
% Foxp3+ cells among CD8-CD4+ cells
E
Th1
% Foxp3-T-bet+ cells among CD8-CD4+ cells
F
Th17
% Foxp3-RORγt+ cells among CD8-CD4+ cells
G
T-bet+ Tregs
% Foxp3+T-bet+ cells among CD8-CD4+ cells
H
RORγt+ Tregs
% Foxp3+RORγt+ cells among CD8-CD4+ cells
I
CD25+ Tregs
% Foxp3+CD25+ cells among CD8-CD4+ cells
J
CD44+ST2+ Tregs
% CD44+ST2+ cells among CD4+Foxp3+ cells
pLNs
Spleen
mLNs
SI
PPs
Colon
VAT
Lung
Liver
Acsbg1+/+
Acsbg1-/-

Supplementary Figure 2. Immunological changes induced by *Acsbg1* deficiency persist in aged mice. Summary plots of immunophenotyping performed in pLNs, spleen, mLNs, SI, PPs, colon, VAT, lung and liver of >80 week old *Acsbg1*$^{-/-}$ mice and *Acsbg1*$^{+/+}$ littermate controls. Frequencies of **(A)** CD44^{-}CD62L^{+} naïve, **(B)** CD44^{+}CD62L^{-} effector, **(C)** Foxp3^{-} Tconv, **(D)** Foxp3^{+} Tregs, **(E)** Foxp3^{-}T-bet^{+} Th1 cells, **(F)** Foxp3^{-}RORγt^{+} Th17 cells, **(G)** T-bet^{+} Tregs (Foxp3^{+}T-bet^{+}), **(H)** RORγt^{+} Tregs (Foxp3^{+}RORγt^{+}) and **(I)** CD25^{+}Foxp3^{+} Tregs among CD8^{-}CD4^{+} T cells. **(J)** Frequency of CD44^{+}ST2^{+} cells among Tregs. Each symbol represents a single mouse. Data are presented as mean ± SEM. Results were pooled from 6 independent experiments with 4-10 mice per experimental group. Significance of differences between means was assessed by ordinary two-way ANOVA with Šídák's multiple comparison test (mean ± 95% CI; **P*<0.05, ***P*<0.01, ****P*<0.001).

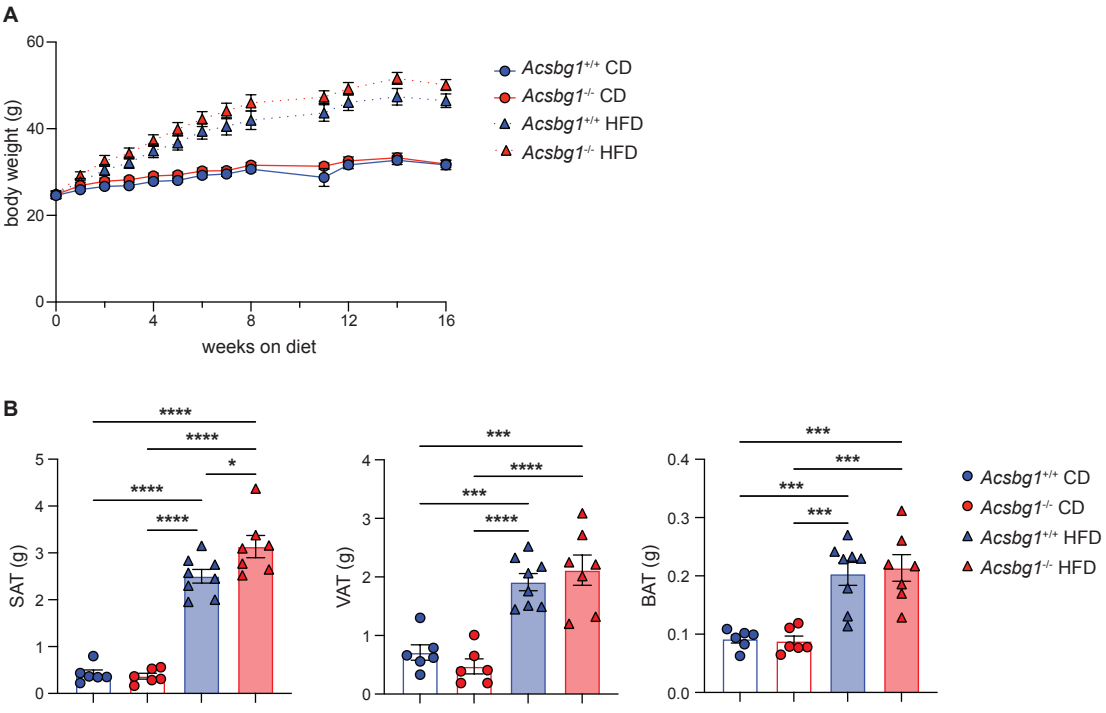
A
body weight (g)
weeks on diet
Acsbg1+/+ CD
Acsbg1-/- CD
Acsbg1+/+ HFD
Acsbg1-/- HFD
B
SAT (g)
VAT (g)
BAT (g)
Acsbg1+/+ CD
Acsbg1-/- CD
Acsbg1+/+ HFD
Acsbg1-/- HFD

Supplementary Figure 3. *Acsbg1* deficiency increases SAT mass under HFD without affecting overall body weight. Male *Acsbg1*$^{+/+}$ and *Acsbg1*$^{-/-}$ mice were challenged as described in Figure 4. **(A)** Body weight was monitored for 16 weeks. **(B)** Then, mice were sacrificed, and SAT, VAT, and BAT were collected and weighed. Each symbol represents a single mouse. Data are presented as mean ± SEM. Data are pooled from 2 independent experiments with 5-14 mice per experimental group. Significance of differences between means was assessed by ordinary two-way ANOVA with Tukey's multiple comparison test (mean ± 95% CI; *P<0.05, **P<0.01, ***P<0.001).

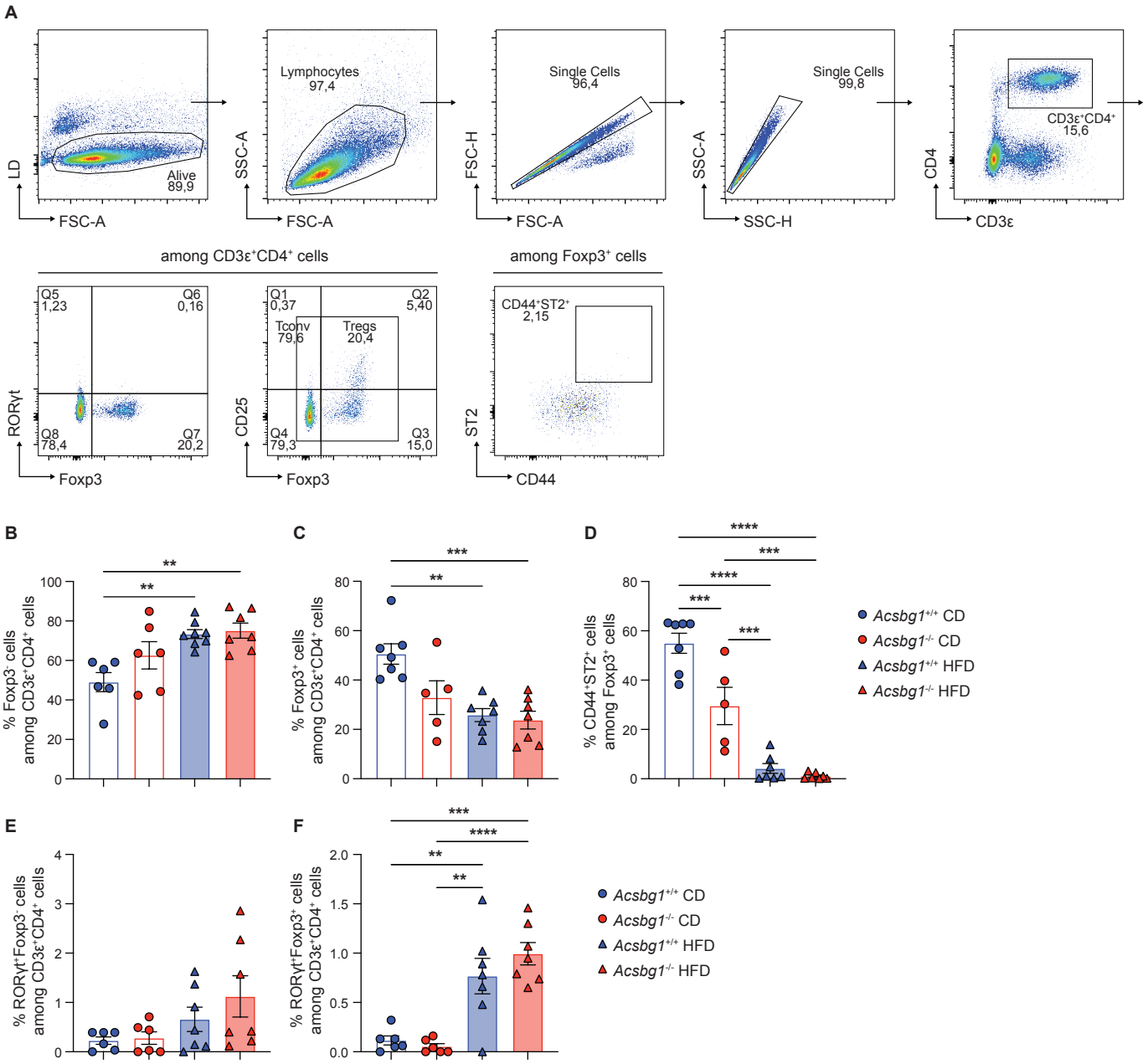
A
LD
FSC-A
Alive
89,9
SSC-A
FSC-A
Lymphocytes
97,4
FSC-H
FSC-A
Single Cells
96,4
SSC-A
SSC-H
Single Cells
99,8
CD4
CD3ε
CD3ε+CD4+
15,6
among CD3ε+CD4+ cells
RORγt
Foxp3
Q5
1,23
Q6
0,16
Q8
78,4
Q7
20,2
CD25
Foxp3
Q1
0,37
Q2
5,40
Tconv
79,6
Tregs
20,4
Q4
79,3
Q3
15,0
among Foxp3+ cells
ST2
CD44
CD44+ST2+
2,15
B
% Foxp3- cells
among CD3ε+CD4+ cells
C
% Foxp3+ cells
among CD3ε+CD4+ cells
D
% CD44+ST2+ cells
among Foxp3+ cells
Acsbg1+/+ CD
Acsbg1-/- CD
Acsbg1+/+ HFD
Acsbg1-/- HFD
E
% RORγt+Foxp3- cells
among CD3ε+CD4+ cells
F
% RORγt+Foxp3+ cells
among CD3ε+CD4+ cells
Acsbg1+/+ CD
Acsbg1-/- CD
Acsbg1+/+ HFD
Acsbg1-/- HFD

Supplementary Figure 4. HFD induces Tconv expansion and reduction of CD44$^+$ST2$^+$ Tregs in VAT, independent of *Acsbg1* genotype. Male *Acsbg1*$^{+/+}$ and *Acsbg1*$^{-/-}$ mice were challenged as described in Figure 4. **(A)** Representative gating strategy used to identify Th17, Tconv, Tregs, RORγt$^+$ and CD44$^+$ST2$^+$ Tregs. **(B-F)** Summary graphs of immunophenotyping performed in VAT. Frequencies of **(B)** Tconv, **(C)** Tregs among CD3e$^+$CD4$^+$ cells. **(D)** Frequencies of CD44$^+$ST2$^+$ cells among Tregs. Frequencies of **(E)** Foxp3$^-$RORγt$^+$ Th17 cells, **(F)** RORγt$^+$ Tregs among CD3e$^+$CD4$^+$ cells. Each symbol represents a single mouse. Data are presented as mean ± SEM. Results were pooled from 6 independent experiments with 5-8 mice per experimental group. Significance of differences between means was assessed by ordinary two-way ANOVA with Šídák's multiple comparison test (mean ± 95% CI; *P<0.05, **P<0.01, ***P<0.001).

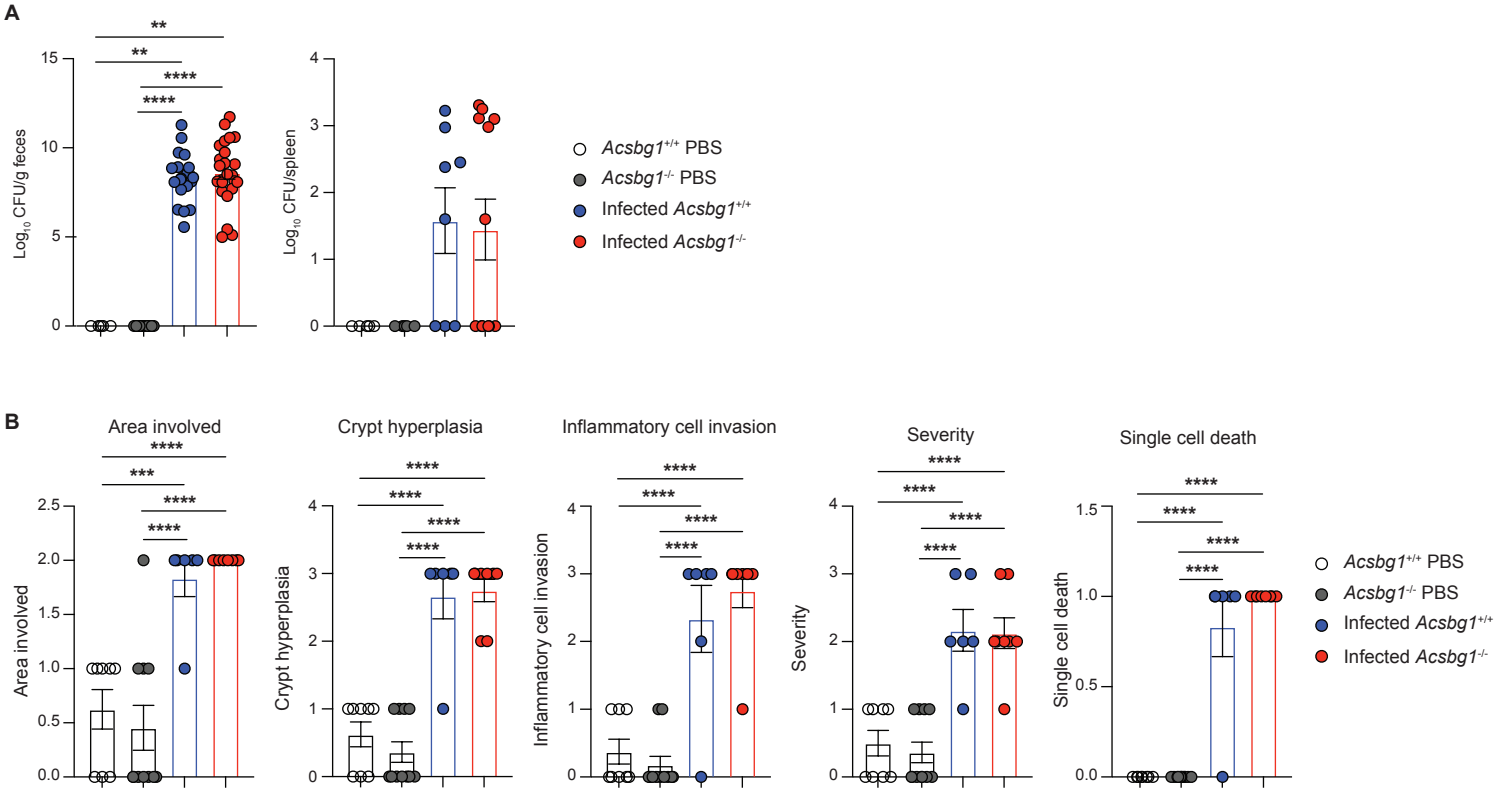
A
Log10 CFU/g feces
Log10 CFU/spleen
Acsbg1+/+ PBS
Acsbg1-/- PBS
Infected Acsbg1+/+
Infected Acsbg1-/-
B
Area involved
Crypt hyperplasia
Inflammatory cell invasion
Severity
Single cell death

Supplementary Figure 5. Comparable bacterial burden at 7 dpi and colitis at 14 dpi in *Acsbg1*$^{-/-}$ mice and *Acsbg1*$^{+/+}$ mice following *C. rodentium* infection. *Acsbg1*$^{-/-}$ mice and *Acsbg1*$^{+/+}$ littermate controls were infected as described in Figure 4. Mice were sacrificed at either 7 or 14 dpi. **(A)** CFU of bacteria recovered from feces (left) and spleen collected at 7 dpi (right). **(B)** At 14 dpi, colon inflammation was assessed by histological analysis after H&E staining. Scatter plots with bars show the area involved, crypt hyperplasia, inflammatory cell invasion, severity of inflammation and single cell death. Each symbol represents a single mouse. Data are presented as mean ± SEM. Results were pooled from **(A)** 9 independent experiments (n = 4-13 biological replicates per group in total). Significance of differences between means was assessed by ordinary two-way ANOVA with Tukey's multiple comparison test (mean ± 95% CI; **P*<0.05, ***P*<0.01, ****P*<0.001).

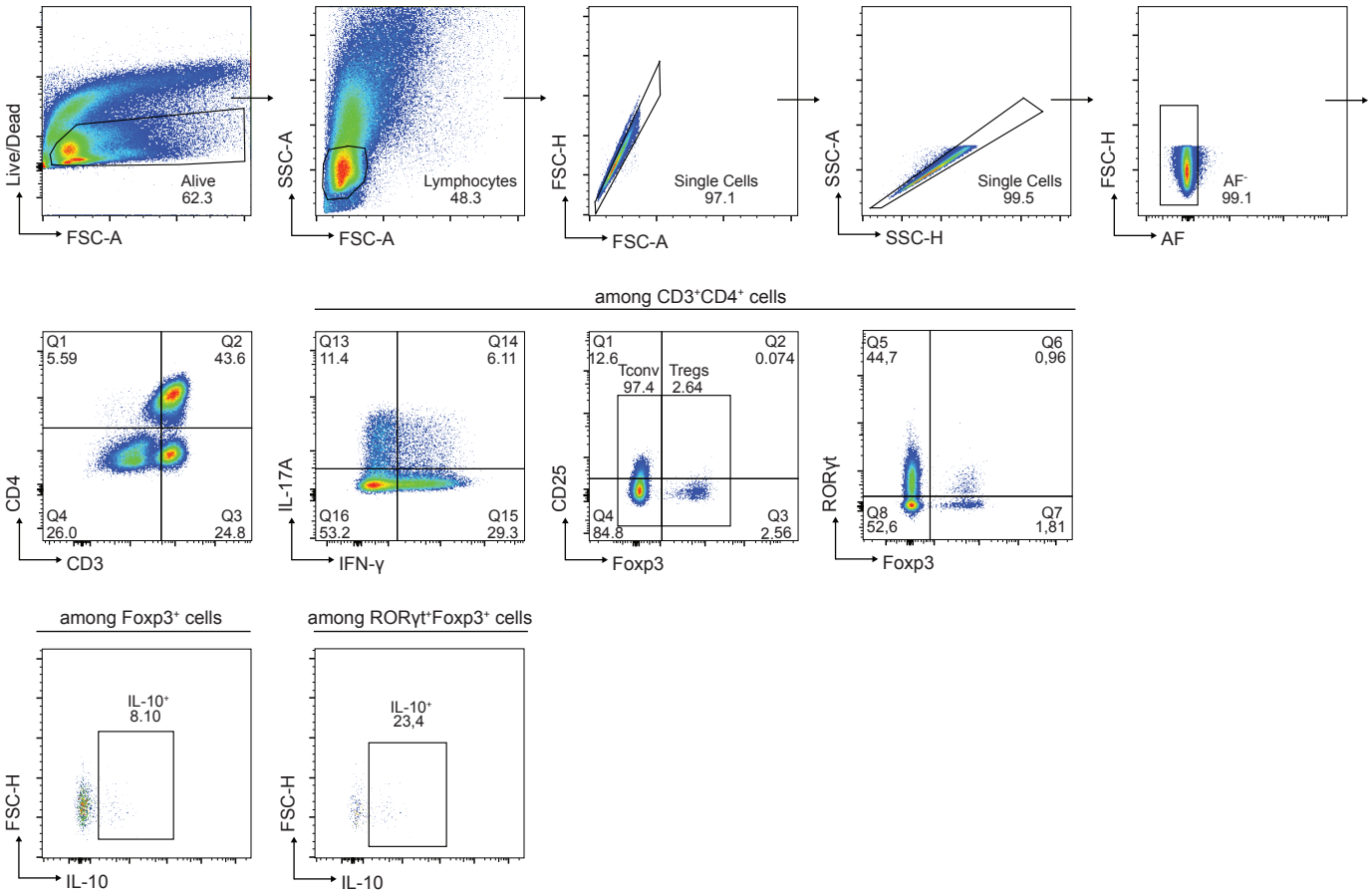
Live/Dead
FSC-A
Alive
62.3
SSC-A
FSC-A
Lymphocytes
48.3
FSC-H
FSC-A
Single Cells
97.1
SSC-A
SSC-H
Single Cells
99.5
FSC-H
AF
AF-
99.1
among CD3+CD4+ cells
CD4
CD3
Q1
5.59
Q2
43.6
Q4
26.0
Q3
24.8
IL-17A
IFN-γ
Q13
11.4
Q14
6.11
Q16
53.2
Q15
29.3
CD25
Foxp3
Q1
12.6
Tconv
97.4
Tregs
2.64
Q2
0.074
Q4
84.8
Q3
2,56
RORγt
Foxp3
Q5
44,7
Q6
0,96
Q8
52,6
Q7
1,81
among Foxp3+ cells
FSC-H
IL-10
IL-10+
8.10
among RORγt+Foxp3+ cells
FSC-H
IL-10
IL-10+
23,4

Supplementary Figure 6. Flow cytometry analysis of colon samples following *C. rodentium* infection. *Acsbg1*$^{-/-}$ mice and *Acsbg1*$^{+/+}$ littermate controls were infected as described in Figure 3. At 14 dpi, mice were sacrificed and colon samples were collected and analyzed by flow cytometry. **(A)** Gating strategy for cytokine detection. Isolated cells were stimulated *in vitro* with PMA, ionomycin and brefeldin A for 4 h at 37°C. Live/Dead discrimination was performed using the LIVE/DEAD Fixable Blue Dead Cell stain. Live cells were gated according to the forward scatter (FSC) and side scatter (SSC) area parameters. Doublet exclusion was then performed using the height (H) versus width (W) parameters of FSC and SSC, respectively. Among the single cells, CD3^{+}CD4^{+} cells were gated to identify CD4^{+} T cells. IL-17A^{-}IFN-γ^{+}, IL-17A^{+}IFN-γ^{-} and IL-17A^{+}IFN-γ^{+} cells were gated to identify single- or double-producing cells among CD4^{+} T cells. According to the expression of Foxp3, CD4^{+} T cells were subdivided into Foxp3^{+} Tregs and Foxp3^{-} Tconv cells. IL-10^{+} cells were gated to identify IL-10-producing cells among Foxp3^{+} Tregs and RORγt^{+}Foxp3^{+} Tregs.

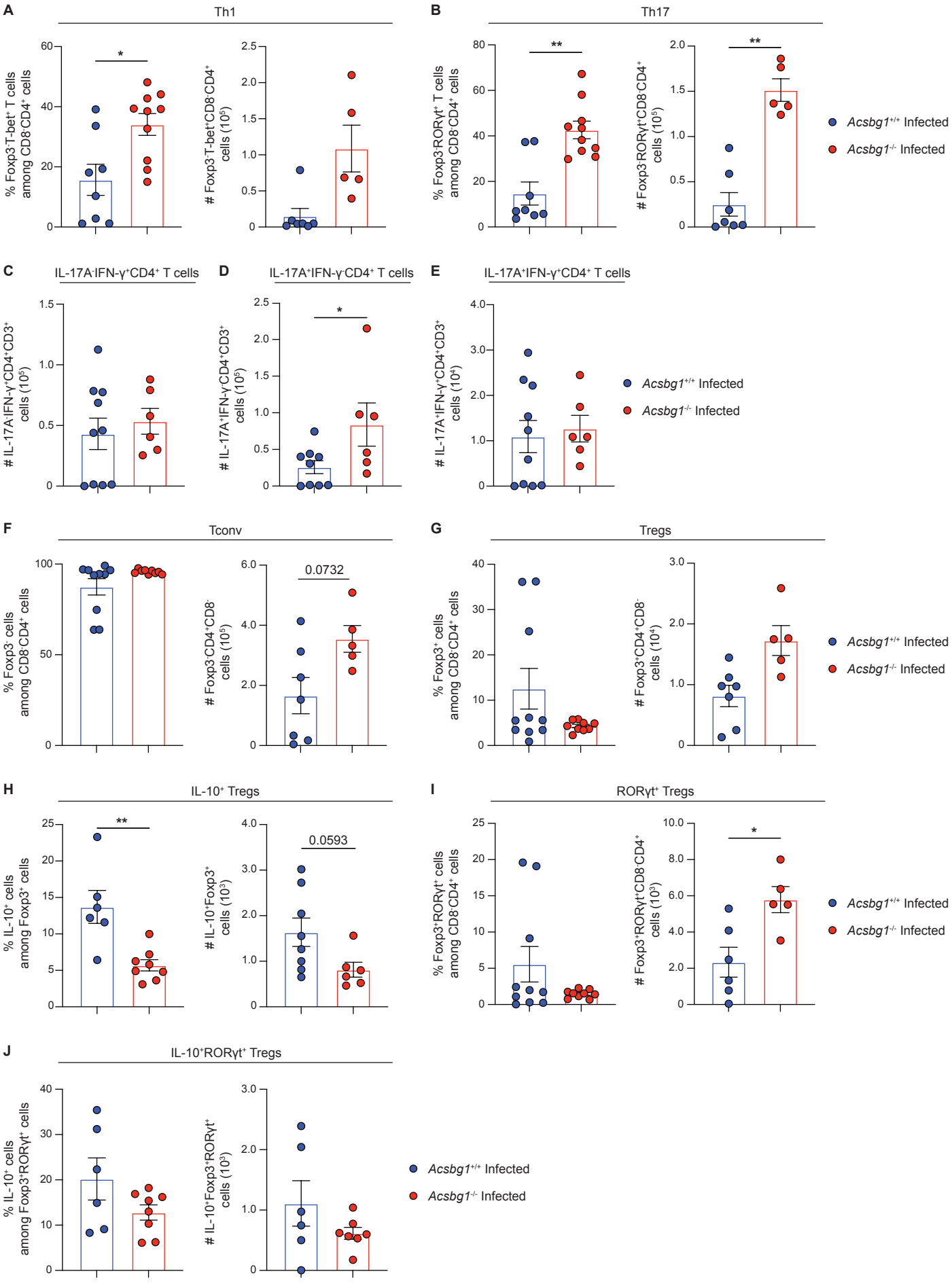
A
Th1
% Foxp3⁻T-bet⁺ T cells among CD8⁻CD4⁺ cells
# Foxp3⁻T-bet⁺CD8⁻CD4⁺ cells (10⁵)
B
Th17
% Foxp3⁻RORγt⁺ T cells among CD8⁻CD4⁺ cells
# Foxp3⁻RORγt⁺CD8⁻CD4⁺ cells (10⁵)
Acsbg1+/+ Infected
Acsbg1-/- Infected
C
IL-17A⁻IFN-γ⁺CD4⁺ T cells
IL-17A⁻IFN-γ⁺CD4⁺CD3⁺ cells (10⁵)
D
IL-17A⁺IFN-γ⁻CD4⁺ T cells
IL-17A⁺IFN-γ⁻CD4⁺CD3⁺ cells (10⁵)
E
IL-17A⁺IFN-γ⁺CD4⁺ T cells
IL-17A⁺IFN-γ⁺CD4⁺CD3⁺ cells (10⁴)
F
Tconv
% Foxp3⁻ cells among CD8⁻CD4⁺ cells
# Foxp3⁻CD4⁺CD8⁻ cells (10⁵)
0.0732
G
Tregs
% Foxp3⁺ cells among CD8⁻CD4⁺ cells
# Foxp3⁺CD4⁺CD8⁻ cells (10⁴)
H
IL-10⁺ Tregs
% IL-10⁺ cells among Foxp3⁺ cells
# IL-10⁺Foxp3⁺ cells (10³)
0.0593
I
RORγt⁺ Tregs
% Foxp3⁺RORγt⁺ cells among CD8⁻CD4⁺ cells
# Foxp3⁺RORγt⁺CD8⁻CD4⁺ cells (10³)
J
IL-10⁺RORγt⁺ Tregs
% IL-10⁺ cells among Foxp3⁺RORγt⁺ cells
# IL-10⁺Foxp3⁺RORγt⁺ cells (10³)

Supplementary Figure 7. *Acsbg1* deficiency exacerbates *C. rodentium* infection by affecting Th1 cells, Th17 cells and Tregs. *Acsbg1*$^{-/-}$ mice and *Acsbg1*$^{+/+}$ littermate controls were infected as described in Figure 3. At 14 dpi, mice were sacrificed and colon samples were collected and analyzed by flow cytometry. **(A-J)** Summary plots showing frequencies and absolute numbers of **(A)** Foxp3^{-}T-bet^{+} Th1 cells and **(B)** Foxp3^{-}RORγt^{+} Th17 cells among CD8^{-}CD4^{+} T cells. Absolute numbers of **(C)** IL-17A^{-}IFN-γ^{+}, **(D)** IL-17A^{+}IFN-γ^{-} and **(E)** IL-17A^{+}IFN-γ^{+} cells among CD3^{+}CD4^{+} T cells. Frequencies and absolute numbers of **(F)** Foxp3^{-} Tconv and **(G)** Foxp3^{+} Tregs among CD8^{-}CD4^{+} T cells. Frequencies and absolute numbers of **(H)** IL-10^{+} cells among Foxp3^{+} Tregs. **(I)** Frequencies and absolute numbers of RORγt^{+} Tregs among CD3^{+}CD4^{+} T cells. **(J)** Frequencies and absolute numbers of IL-10^{+} cells among RORγt^{+} Tregs. Each symbol represents a single mouse. Data are presented as mean ± SEM. Results were pooled from 4 independent experiments with 6-12 mice per experimental group. Significance of differences between means was assessed by non-parametric Mann-Whitney test (mean ± 95% CI; **P*<0.05, ***P*<0.01, ****P*<0.001).

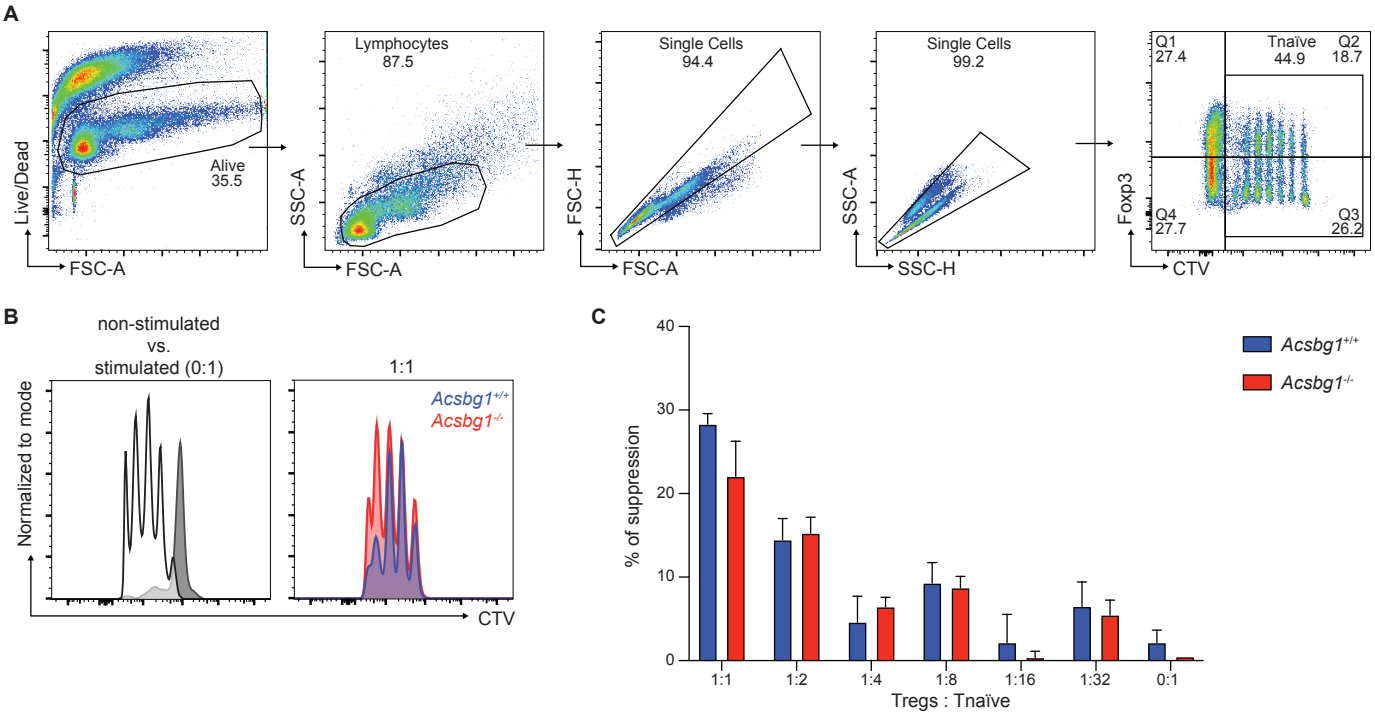
A
Live/Dead
FSC-A
Alive
35.5
SSC-A
FSC-A
Lymphocytes
87.5
FSC-H
FSC-A
Single Cells
94.4
SSC-A
SSC-H
Single Cells
99.2
Foxp3
CTV
Q1
27.4
Tnaïve
44.9
Q2
18.7
Q4
27.7
Q3
26.2
B
non-stimulated
vs.
stimulated (0:1)
1:1
Normalized to mode
CTV
Acsbg1+/+
Acsbg1-/-
C
% of suppression
Tregs : Tnaïve
1:1
1:2
1:4
1:8
1:16
1:32
0:1
Acsbg1+/+
Acsbg1-/-

Supplementary Figure 8. *Acsbg1* deficiency moderately reduces the suppressive capacity of Tregs *in vitro*. (A) Exemplary gating strategy to identify Tnaive from the *in vitro* suppression assay. **(B)** Histogram plots showing the distribution of CTV-labeled Tnaïve with (white) and without (grey) stimulus as well as co-cultures with *Acsbg1*$^{+/+}$ (blue) or *Acsbg1*$^{-/-}$ (red) Tregs (ratio 1:1). **(C)** Bar graph summarizing the percentage of suppression of CTV-labelled effector T cells in the indicated Treg/Tnaïve co-cultures, including also non-stimulated (ns) Tnaïve. Data are presented as mean ± SEM. Symbols represent technical replicates of 2-3 independent experiments. Significance was assessed by ordinary two-way ANOVA with Šidák's multiple comparison test (mean ± 95% CI; $^{**}p < 0.01$ and $^{***}p < 0.001$).

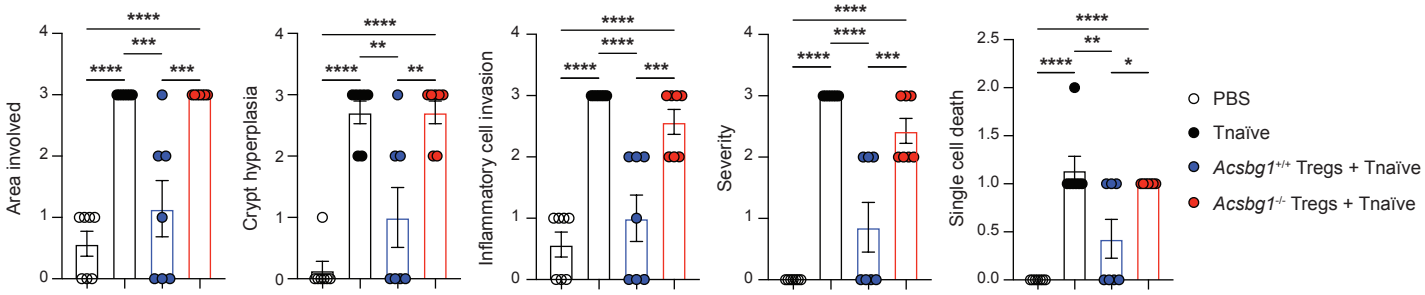
Area involved
Crypt hyperplasia
Inflammatory cell invasion
Severity
Single cell death
PBS
Tnaïve
Acsbg1+/+ Tregs + Tnaïve
Acsbg1-/- Tregs + Tnaïve

Supplementary Figure 9. Enhanced colitis in mice receiving *Acsbg1*$^{-/-}$ Tregs compared to *Acsbg1*$^{+/+}$ Tregs. Indicated Tregs and Tnaïve were adoptively co-transferred in a 1:4 ratio into sex- and age-matched *Rag2*$^{-/-}$ mice by i.p. injection. Control groups received the same amount of Tnaïve alone or PBS. Eight weeks after transfer, colon inflammation was assessed by histological analysis. Scatter plots with bars show the area involved, crypt hyperplasia, inflammatory cell invasion, severity of inflammation and single cell death. Each symbol represents a single mouse. Data are presented as mean ± SEM. Results were pooled from 4 independent experiments with 7 mice per experimental group. Significance of differences between means was assessed by ordinary two-way ANOVA with Tukey's multiple comparison test (mean ± 95% CI; **P*<0.05, ***P*<0.01, ****P*<0.001).

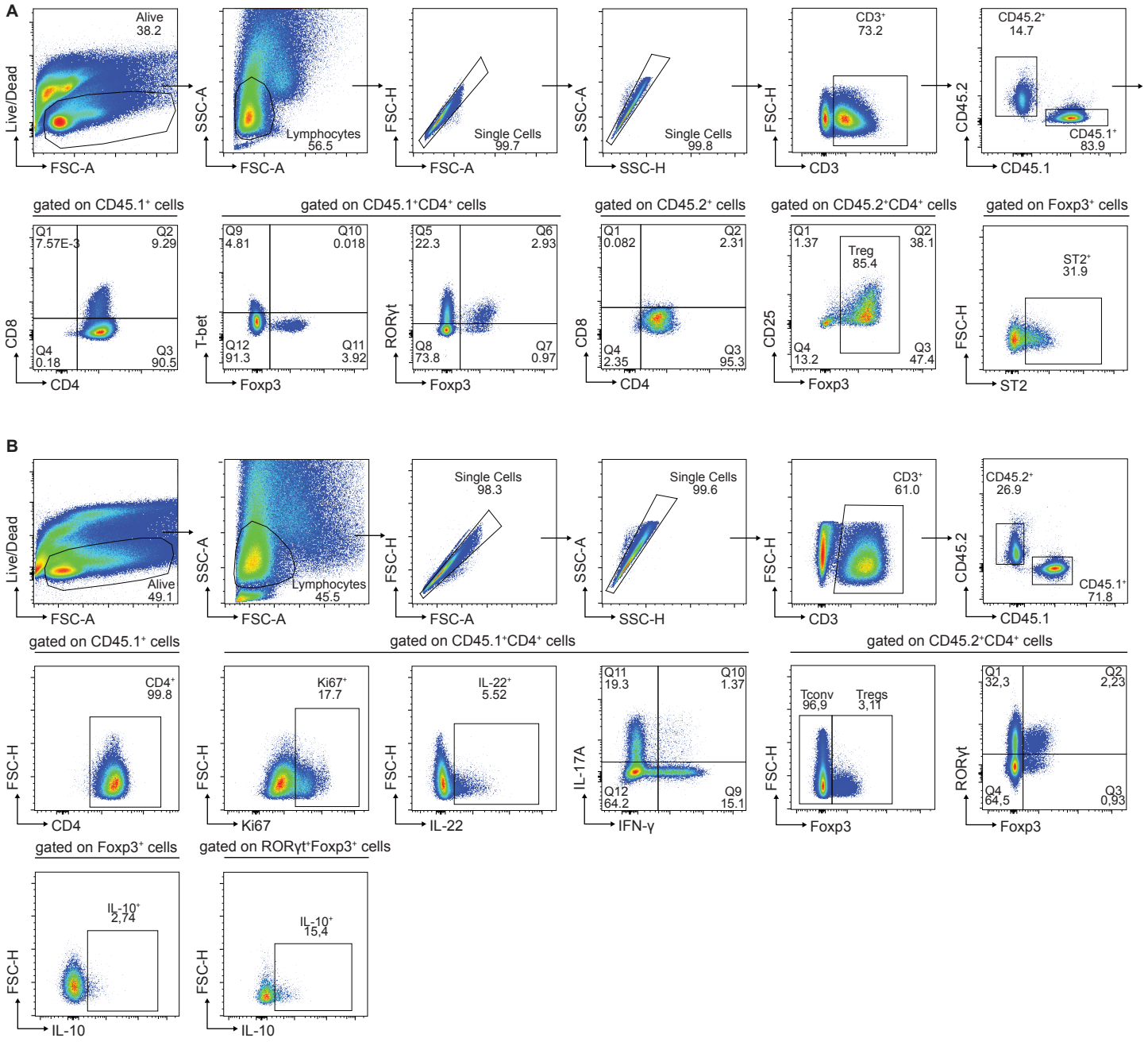
A
Live/Dead
FSC-A
Alive
38.2
SSC-A
FSC-A
Lymphocytes
56.5
FSC-H
FSC-A
Single Cells
99.7
SSC-A
SSC-H
Single Cells
99.8
FSC-H
CD3
CD3+
73.2
CD45.2
CD45.1
CD45.2+
14.7
CD45.1+
83.9
gated on CD45.1+ cells
CD8
CD4
Q1
7.57E-3
Q2
9.29
Q4
0.18
Q3
90.5
gated on CD45.1+CD4+ cells
T-bet
Foxp3
Q9
4.81
Q10
0.018
Q12
91.3
Q11
3.92
RORγt
Foxp3
Q5
22.3
Q6
2.93
Q8
73.8
Q7
0.97
gated on CD45.2+ cells
CD8
CD4
Q1
0.082
Q2
2.31
Q4
2.35
Q3
95.3
gated on CD45.2+CD4+ cells
CD25
Foxp3
Q1
1.37
Q2
38.1
Treg
85.4
Q4
13.2
Q3
47.4
gated on Foxp3+ cells
FSC-H
ST2
ST2+
31.9
B
Live/Dead
FSC-A
Alive
49.1
SSC-A
FSC-A
Lymphocytes
45.5
FSC-H
FSC-A
Single Cells
98.3
SSC-A
SSC-H
Single Cells
99.6
FSC-H
CD3
CD3+
61.0
CD45.2
CD45.1
CD45.2+
26.9
CD45.1+
71.8
gated on CD45.1+ cells
FSC-H
CD4
CD4+
99.8
gated on CD45.1+CD4+ cells
FSC-H
Ki67
Ki67+
17.7
FSC-H
IL-22
IL-22+
5.52
IL-17A
IFN-γ
Q11
19.3
Q10
1.37
Q12
64.2
Q9
15.1
gated on CD45.2+CD4+ cells
FSC-H
Foxp3
Tconv
96,9
Tregs
3,11
RORγt
Foxp3
Q1
32,3
Q2
2,23
Q4
64,5
Q3
0,93
gated on Foxp3+ cells
FSC-H
IL-10
IL-10+
2,74
gated on RORγt+Foxp3+ cells
FSC-H
IL-10
IL-10+
15,4

Supplementary Figure 10. Gating strategies for immunophenotyping of mice from adoptive transfer colitis experiments. (A) Exemplary gating strategy used to identify different $CD4^+$ T cell subsets among $CD45.1^+CD4^+$ T cells, and $Foxp3^+$ Tregs among $CD45.2^+CD4^+$ T cells. **(B)** Exemplary gating strategy used to identify $Ki67^+$, $IL\text{-}22^+$, $IL\text{-}17A^+$, $IFN\text{-}\gamma^+$ and $IL\text{-}17A^+IFN\text{-}\gamma^+$ cells among $CD45.1^+CD4^+$ T cells, as well as $IL\text{-}10^+$ cells among Tregs and $ROR\gamma t^+$ Tregs.

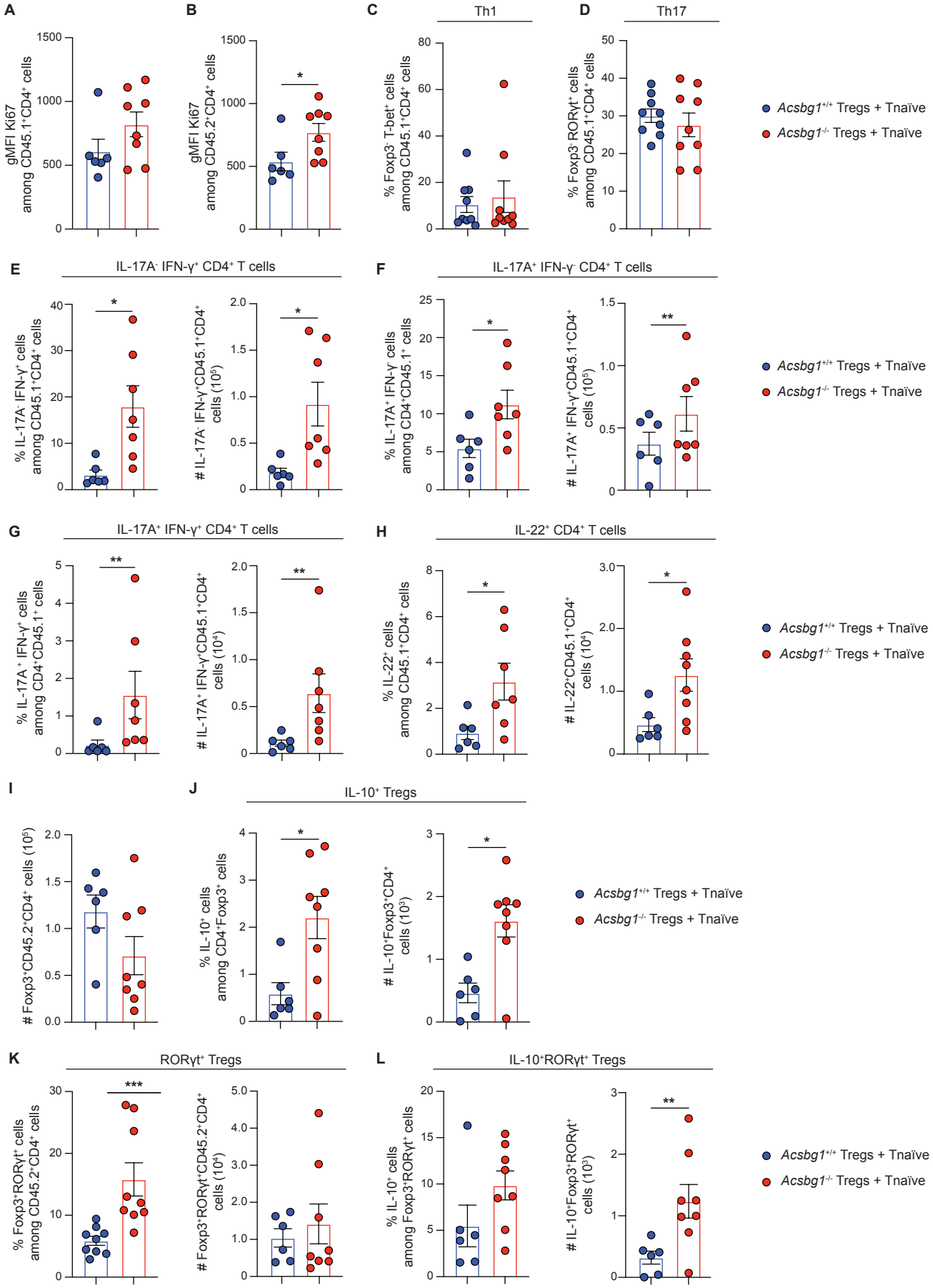
A
gMFI Ki67 among CD45.1+CD4+ cells
B
gMFI Ki67 among CD45.2+CD4+ cells
C
Th1
% Foxp3- T-bet+ cells among CD45.1+CD4+ cells
D
Th17
% Foxp3- RORγt+ cells among CD45.1+CD4+ cells
Acsbg1+/+ Tregs + Tnaïve
Acsbg1-/- Tregs + Tnaïve
E
IL-17A- IFN-γ+ CD4+ T cells
% IL-17A- IFN-γ+ cells among CD45.1+CD4+ cells
# IL-17A- IFN-γ+CD45.1+CD4+ cells (10^5)
F
IL-17A+ IFN-γ- CD4+ T cells
% IL-17A+ IFN-γ- cells among CD4+CD45.1+ cells
# IL-17A+ IFN-γ+CD45.1+CD4+ cells (10^5)
G
IL-17A+ IFN-γ+ CD4+ T cells
% IL-17A+ IFN-γ+ cells among CD4+CD45.1+ cells
# IL-17A+ IFN-γ+CD45.1+CD4+ cells (10^4)
H
IL-22+ CD4+ T cells
% IL-22+ cells among CD45.1+CD4+ cells
# IL-22+CD45.1+CD4+ cells (10^4)
I
Foxp3+CD45.2+CD4+ cells (10^5)
J
IL-10+ Tregs
% IL-10+ cells among CD4+Foxp3+ cells
# IL-10+Foxp3+CD4+ cells (10^3)
K
RORγt+ Tregs
% Foxp3+RORγt+ cells among CD45.2+CD4+ cells
# Foxp3+RORγt+CD45.2+CD4+ cells (10^4)
L
IL-10+RORγt+ Tregs
% IL-10+ cells among Foxp3+RORγt+ cells
# IL-10+Foxp3+RORγt+ cells (10^3)

Supplementary Figure 11. *Acsbg1*$^{-/-}$ Tregs fail to attenuate T-cell mediated intestinal inflammation. Tnaïve (Lin^{-}CD4^{+}hCD2^{-}CD25^{-}CD62L^{high}) were sorted from Foxp3^{hCD2} mice (CD45.1), whereas Tregs (Lin^{-}CD4^{+}CD25^{high}) were sorted from *Acsbg1*$^{-/-}$ mice or *Acsbg1*$^{+/+}$ littermate controls (CD45.2). Tregs and Tnaïve were adoptively co-transferred in a 1:4 ratio into sex- and age-matched *Rag2*$^{-/-}$ mice by i.p. injection. Control groups received the same amount of Tnaïve alone or PBS. Eight weeks after adoptive transfer, mice were sacrificed and colon samples analyzed by flow cytometry. gMFI of Ki67 among **(A)** CD45.1^{+}CD4^{+} and **(B)** CD45.2^{+}CD4^{+} T cells. Frequencies of **(C)** Th1 and **(D)** Th17 cells among CD45.1^{+}CD4^{+} T cells. Frequencies and absolute cell numbers of **(E)** IFNγ^{+}IL-17A^{-}, **(F)** IFNγ^{-}IL-17A^{+}, **(G)** IFNγ^{+}IL-17A^{+} and **(H)** IL-22^{+} cells among CD45.1^{+}CD4^{+} T cells. **(I)** Absolute numbers of Tregs among CD45.2^{+}CD4^{+} cells. **(J-K)** Frequency and absolute numbers of **(J)** IL-10^{+} and **(K)** RORγt^{+} cells among Tregs. **(L)** Frequency and absolute number of IL-10^{+} cells among RORγt^{+} Tregs. Each symbol represents a single mouse. Data are presented as mean ± SEM. Results were pooled from 2 independent experiments with 9 mice per experimental group. Significance of differences between means was assessed by non-parametric Mann-Whitney test (mean ± 95% CI; **P*<0.05, ***P*<0.01, ****P*<0.001).